Taylor & Francis
Taylor & Francis Group

RESEARCH PAPER

🔓 OPEN ACCESS | Check for updates

Automated approach for the evaluation of glutathione-S-transferase P1-1 inhibition by organometallic anticancer compounds

Sarah A. P. Pereira[a], A. Catarina Baptista L[a], Lorenzo Biancalana[b], Fabio Marchetti[b], Paul J. Dyson[c] and M. Lúcia M. F. S. Saraiva[a]

[a]LAQV, REQUIMTE, Departamento de Ciências Químicas, Faculdade de Farmácia, Universidade do Porto, Porto, Portugal; [b]Dipartimento di Chimica e Chimica Industriale, Università di Pisa, Pisa, Italy; [c]Institut des Sciences et Ingénierie Chimiques, École Polytechnique Fédérale de Lausanne (EPFL), Lausanne, Switzerland

ABSTRACT

A novel automated method based on sequential injection analysis (SIA), a non-segmented flow injection technique, was developed to evaluate glutathione S-transferase P1-1 (GST P1-1) activity in the presence of organometallic complexes with putative anticancer activity. The assay is based on the reaction of L-glutathione (GSH) and 1-chloro-2,4-dinitrobenzene (CDNB) in the presence of GST P1-1 to afford the GS-DNB conjugate and the reaction may be monitored by an increase in absorbance at 340 nm. A series of ruthenium, iron, osmium and iridium complexes were evaluated as GST P1-1 inhibitors by evaluating their half-maximal inhibitory concentration (IC_{50}). An iridium compound displays the lowest IC_{50} value of $6.7 \pm 0.7\,\mu M$ and an iron compound displays the highest IC_{50} value of $275 \pm 9\,\mu M$. The SIA method is simple to use, robust, reliable, and efficient and uses fewer reagents than batch methods and each analysis takes only 5 minutes.

GRAPHICAL ABSTRACT
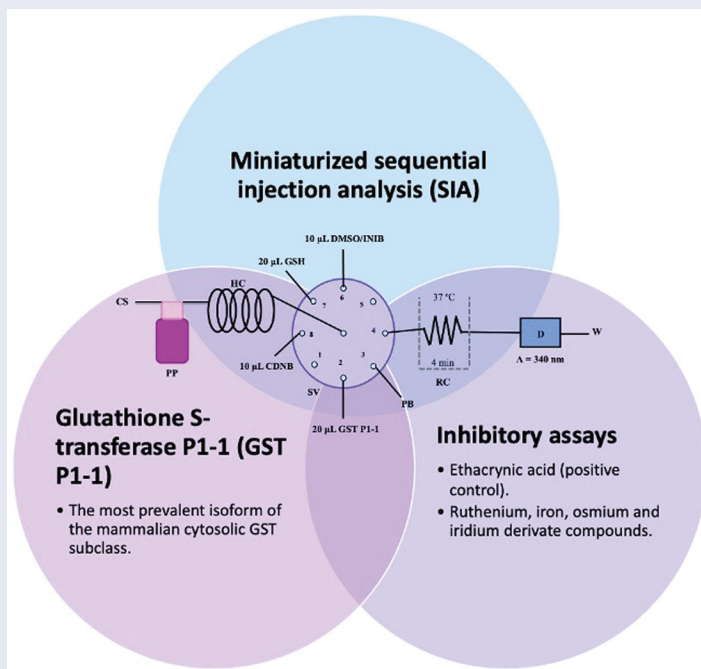
1. Introduction

Glutathione S-transferases (GSTs) are a superfamily broadly distributed in phase II metabolism enzymes that catalyse the conjugation of extensive diversity of reactive electrophiles to the nucleophilic sulphur atom of tripeptide glutathione (γ-L-glutamyl-L-cysteinyl glycine, GSH). After formed, the hydrophilic GSH

conjugates are successfully removed from the cell, inducing the detoxification of the organism[1,2]. The greatest predominant iso-form of the GST subclass in mammalian cytosolic is GST P1-1, and its overexpression can be directly correlated to carcinogenesis and chemotherapeutic drug resistance[3,4]. This isoform is overexpressed in human tumours such as ovarian, kidney, and breast carcin-oma[5,6], with its overexpression accelerating drug metabolism lead-ing to a decrease in therapeutic efficacy[7].

Several GST inhibition batch assays have been reported resort-ing to a different mode of detection, such as an electrochemical assay using a glassy carbon electrode with differential pulse vol-tammetry to evaluate GST kinetic parameters[8], or an immunocyto-chemistry technique to evaluate the cellular reactivity of GSTπ[9]. With a higher level of mechanisation, a high-resolution screening (HRS) technique using two simultaneous enzyme affinity detection (EAD) systems for human GST P1-1 using reverse-phase high-per-formance liquid chromatography (HPLC). This system was first optimised and validated using a flow injection analysis (FIA) sys-tem and the optimised results were then used in HPLC mode[10].

In this work, a sequential injection analysis (SIA) system was developed to assess GST P1-1 activity and evaluate several organometallic compounds with putative anticancer activity. SIA was chosen rather than FIA, as it is better suited to high-cost enzymes/reagents and complicated multi-step reactions since it is possible to use fewer volumes and present several reagents han-dling abilities[11] and minimises some of the drawbacks of batch assays by ensuring effective control of the reaction conditions[12], significantly impacting precision and accuracy[13]. In SIA, enzymatic activity is determined in the early stages of the reaction avoiding interference from low-affinity substrates. Compared to FIA, SIA is more versatile, with computer control mode, and the implementa-tion of different analytical procedures without physical reconfigur-ation of the setting[14].

SIA is an automatic approach that enables the performance of wet-chemistry procedures in a rapid, precise, and efficient manner. SIA systems have been broadly accomplished in the last decades for the application of enzyme-based assays aiming at the evalu-ation of enzyme activity, enzyme inhibition assays, and the deter-mination of specific analytes.

The SIA method reported herein is based on the GST P1-1 cata-lysed reaction of 1-chloro-2,4-dinitrobenzene (CDNB) with reduced glutathione (GSH) which results in an increase in absorbance at 340 nm. Following validation of the assay using ethacrynic acid (EA), a benchmark GST P1-1 inhibitor[15], a selection of organomet-allic iron, ruthenium, osmium, and iridium complexes, currently investigated for their anticancer activity, were tested to evaluate the inhibition capacity against GST P1-1 enzyme. Iron is attractive for developing metal-based drugs due to its bioavailability and the feasible redox chemistry in physiological media[16–18]. Recently, organometallic diiron compounds based on the $\{Fe_2Cp_2(CO)_x\}$

scaffold ($x = 2$ or 3) were shown to display selective cytotoxicity to certain cancer cells. Organoruthenium (half-sandwich) compounds have been extensively studied over the last two decades due to their promising anti-cancer properties[19], with some even validated in vivo against cancers with a very poor prognosis[20,21]. Related osmium and iridium half-sandwich complexes have received far less attention than those of iron and ruthenium concerning their application in medicinal chemistry, but several promising results have been reported[22,23]. The conjugation of known enzyme inhibi-tors to metal-based drugs emerged as a prominent strategy to develop effective anticancer compounds[24], with early examples corresponding to half-sandwich ruthenium complexes modified with EA[25,26], and some of the organometallic compounds studied herein have pendant EA groups[25,27].

2. Materials and methods

2.1. Reagents and solutions

Glutathione S-transferase P1-1 (GST P1-1); 1-Chloro-2,4-dinitroben-zene (CDNB), glutathione (GSH), and ethacrynic acid (EA) were purchased from Sigma. Dimethyl sulfoxide (DMSO) and ethanol were purchased from Merck and Fisher Chemicals, respectively. Ultrapure water obtained from the MILI-Q plus system with a spe-cific conductivity of $< 0.1\ \mu S\ cm^{-1}$ was used to prepare all the solutions.

CDNB and GSH were daily prepared in ethanol and phosphate buffer $0.1\ mol\ L^{-1}$ pH 6.5 at 44 mM and 12 mM, respectively. GST P1 was reconstituted from a solution comprising 50 mM Tris-HCl at pH 7.5 with 50 mM of sodium chloride (NaCl), and 1 mM of 1,4-dithiothreitol (DTT), 5 mM of ethylenediaminetetraacetic acid (EDTA), and 50% of glycerol. The GST P1 solution (0.2 μM) used in the assays was incubated in an ice bath during the procedure. A $0.1\ mol\ L^{-1}$ phosphate buffer solution (pH 6.5) was applied as a carrier solution for the SIA method. Compounds **2a–d**[28], **3a**[29], **4a–d**[30,31], **5a–f**[32–34], **6a–b**[35,36], **7a–e**[37–40] were prepared in agree-ment to literature methods and were dissolved in DMSO.

2.2. Analytical apparatus

The SIA system is represented in Figure 1 and consists of a selec-tion valve Crison® module with 8 ports and a peristaltic pump Gilson® Mini plus 3 sets with a pumping tube of polyvinyl chloride with 1.30 mm i.d. All the system components are connected by Teflon tubes of 0.8 mm in diameter. A reactor coil of 50 cm in length was immersed inside the thermostatic bath to maintain the mixture at 37 °C.

Measurements were performed using a Jenway® 6300 spectro-photometer detector, incorporating an 80 μL flow cell (Hellma Analytics®), connected to the reactor coil, with 10 mm of optical
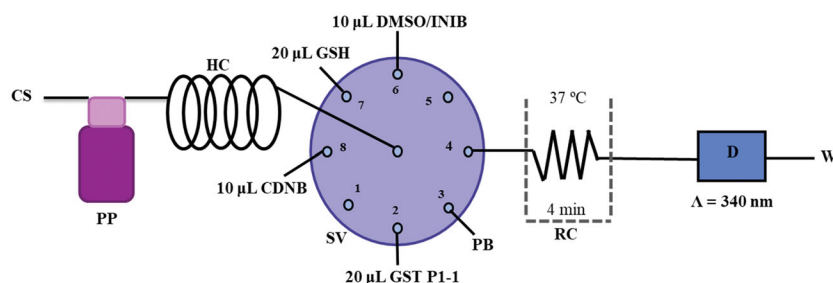

Figure 1. Illustration of the SIA manifold used. CS – Carrier solution; HC – holding coil; PP – peristaltic pump; SV – Selection valve; DMSO/INIB – dimethylsulfoxide/inhibitor; CDNB- 1-Chloro-2,4-dinitrobenzene; GSH – Glutathione reduced; GST P1-1 – Glutathione S-transferase P1-1; PB – Phosphate buffer; RC – Reaction coil; D – Detector and W – Waste.

path length. The absorption wavelength was fixed at 340 nm. Microsoft QuickBasic 4.5 software was used to control the flow system.

2.3. Sequential injection analysis procedure

The half-maximal inhibitory concentration (IC$_{50}$) determination of GST P1-1 activity of the compounds was performed using the SIA system as follows. Before starting the analytical cycle, all the system tubes were filled with the carrier solution (phosphate buffer at pH 6.5). Then the tubes from positions 2, 3, 6, 7, and 8 were filled with GST P1-1, phosphate buffer pH 6.5, inhibitor, GSH, and CDNB, respectively. Afterward, the analytical cycle, presented in Table 1, was carried out by the aspiration of 10 μL of CDNB, 10 μL of DMSO/inhibitor, 20 μL of GST P1-1, and 20 μL of GSH (steps 1–4). Then, the aliquots were propelled to the reaction coil (RC) by flow reversal (step 5) and the flow was stopped inside the RC for 4 min to promote the reaction product formation (step 6). After this stop period, the reaction product was propelled to the detection cell (step 7), and the analytical signal was recorded. All the determinations were carried out at 37 °C and each assay was performed in triplicate.

2.4. Batch procedure

To evaluate the enzymatic reaction, a concentration of GST P1 of 20 nM was spectrophotometrically determined at 340 nm by monitoring the reaction of CDNB (1 mM) with GSH (2 mM) (Figure 2) over 8 min in 0.1 M potassium phosphate buffer at pH 6.5 based on a previously reported protocol[41]. All the assays were performed

at around 37 °C and in triplicate. The IC$_{50}$ values were acquired using GraphPad Prism 7 software.

2.5. Data analysis

The evaluation of the inhibition curves was performed using GraphPad Prism 7 software using the equation defined by [Inhibitor] vs. normalised responsible–variable slope, where X values should be concentrations, not transformed to logarithms and the Y values of the curve were go from 100 down to 0. This model corresponds to the equation $Y = \frac{100}{1+\left(\frac{IC50}{X}\right)^{Hillslope}}$.

To obtain the normalised activities for each inhibitor concentration, we assume that 100% is the maximum activity of the reaction without the presence of an inhibitor. 100% is equal to 1, so each percentage of inhibition is converted into a normalised activity (a number between 0 and 1, being 0 and 1 equal to 0% and 100%).

3. Results and discussion

3.1. Optimisation of the SIA methodology

The first stage of the SIA method development comprised the evaluation of the physical configuration and the chemical factors that affect the reaction. For this, it was used the univariate approach was where each parameter is improved while the others are maintained constant. The main parameters studied include the reaction time, the reagents aliquots volume, their aspiration order, and the temperature. Table 2 lists these optimised parameters with the studied range and the chosen values.

Table 1. Analytical cycle used to perform the GST P1-1 inhibition assays.

Step	Position valve	Reagent	Volume (μL)	Time (s)	Flow rate (mL min^{-1})	Action
1	8	CDNB	10	1.2	0.5	Aspiration of CDNB
2	6	DMSO/ inhibitor	10	1.2	0.5	Aspiration of DMSO/inhibitor
3	2	GST P1-1	20	2.4	0.5	Aspiration of GST P1-1
4	7	GSH	20	2.4	0.5	Aspiration of GSH
5	4	Mixture	333	20	1	Propulsion to the reactor coil
6	4		–	240	0	Stop period in reactor coil
7	4	Mixture	2000	60	2	Propulsion to the detector
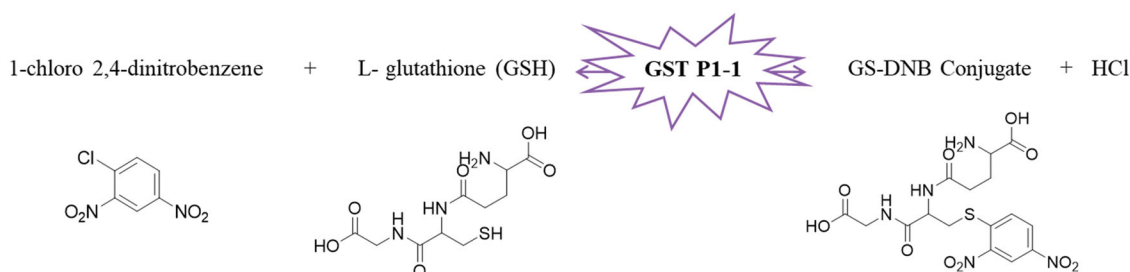
Figure 2. GST P1-1 enzymatic reaction.

Table 2. SIA system optimisation.

Condition	Range	Selected value
Stop period (min)	0–5	4
Aspiration order	GSH – DMSO/inhibitor – GST P1-1 – CDNB	CDNB – DMSO/inhibitor – GST P1-1 – GSH
	GSH – GST P1-1 – DMSO/inhibitor – CDNB	
	CDNB – DMSO/inhibitor – GST P1-1 – GSH	
	CDNB – GST P1-1- DMSO/inhibitor – GSH	
Temperature (°C)	25–37	37
GST volume (μL)	10–25	20
GSH volume (μL)	15–25	20

Figure 3. Optimisation of the GST P1-1 reaction time.

GST P1 activity was evaluated using a flow injection methodology, with a stopped-flow period at the reaction coil, enabling the GS-DNB product development without further increasing the di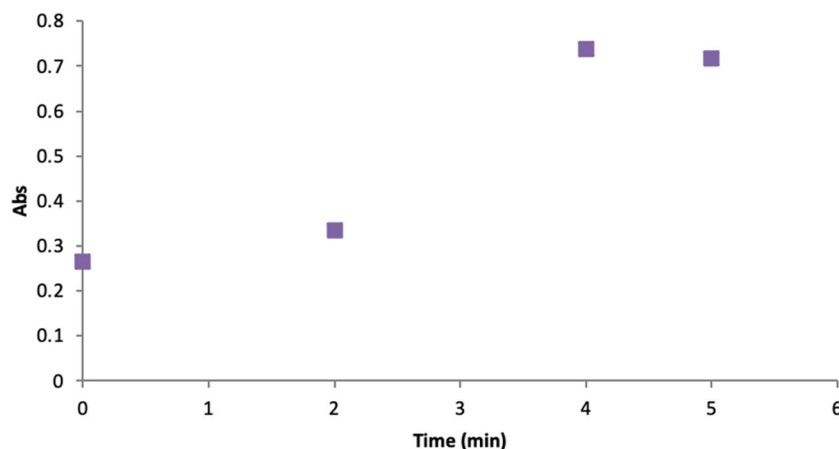spersion. Stop reaction times of 0, 2, 4, and 5 min were assessed with a maximum increase in absorbance after 4 min of stopped time in the reaction coil (Figure 3).

The dispersion of the aliquots is essential for the partial zones overlap and consequent reaction. Also, the aspiration order is very important since the implemented sequence must ensure contact between the enzyme, the substrate, and the cofactor to maximise the chemical reaction. Hence, the aspiration order of the aliquots was also studied. The aspiration order CDNB – DMSO/inhibitor – GST – GSH was selected because the analytical signal is 4.3 times higher than the aspiration order CDNB – GST – DMSO/inhibitor – GSH and 1.7 times higher than the aspiration order GSH – GST – DMSO/inhibitor – CDNB/GSH – DMSO/inhibitor – GST – CDNB. Previously reported GST P1 assays are conducted at either 25 or 37 °C[27,42,43]. To guarantee the best analytical signal and to simulate body temperature, 37 °C was used. Different GSH (12 mM) and GST P1(5×10^{-6} g mL^{-1}) volumes were also tested with 20 µL being optimal for both. The flow rate of the propulsion to the detector was studied between 1- and 2-ml min^{-1}. It is evident that using the higher flow rate (2 ml min^{-1}), we obtained a higher absorbance of the final product (increases 1.5 times).

Using the optimised parameters, the analytical characteristics of the system were determined, to afford the concentration range in which there is a linear relationship between the CDNB concentration and the spectrophotometric signal. A calibration curve was obtained using standard solutions of increasing concentrations of CDNB. The obtained calibration curve was Abs = (0.09 ± 0.02) C (mM) + (0.14 ± 0.02); $R^2 = 0.99$, where Abs and C correspond to the absorbance intensity and the concentration of CDNB in mM, respectively, with a confidence limit for the intercept and slope of 95%. The linearity range of this method is between 0.85 and 44 mM. All the analytical features of this calibration curve are represented in Table 3.

3.2. Determination of GST P1-1 inhibition by organometallic compounds

The optimised GST P1-1 SIA method was used to determine the inhibition profiles of a library of organometallic compounds. Each concentration of each compound was performed in triplicate using a 1.8 mM of CDNB solution which was defined from the linear concentration range of the calibration curve.

Table 3. Analytical features of the calibration curve.

Analytical features	Values
Detection limit	0.26 mM
Quantification limit	0.85 mM
R^2	0.99
Slope	0.09
Intercept	0.14
Standard error of slope (Sb)	0.006
Standard error of intercept (Sa)	0.007
Standard error of regression	0.008
Sum of squares of the regression	0.01
Sum of squares of the residuals	0.0002

In Figure S1 in the Supplementary Material, it is represented the obtained polynomial relations depending on the normalised activity and each compound logarithm concentration. The resulting IC$_{50}$ values of the compounds are given in Table 4. The RSD obtained for all the IC$_{50}$ obtained with the new methods is around 7 ($n = 20$).

The known GST P1-1 inhibitor, ethacrynic acid (see Introduction), was used as a positive control. The literature reports different IC$_{50}$ values for **EA** ranging from 4.9 µM[44] to 12 µM[27], the latter being close to the IC$_{50}$ of 11.3 ± 0.8 µM obtained using the SIA system. The organometallic compounds display IC$_{50}$ values ranging from 6.7 ± 0.7 to 275 ± 9 µM with the results allowing some structure-activity relationships to be ascertained. RAPTA complexes **2a–d** showed a modest GST P1-1 inhibitory activity (average IC$_{50}$ 54 µM), albeit considerably higher than the related Ru(II)-arene compound **3a** (RUCYN, IC$_{50}$ 235 µM). Conjugation of **EA** to the Ru(II) and Os(II) η^6-arene complexes via a modified triaryl phosphine ligand (complexes **7a–c**) does not result in effective GST P1-1 inhibitors with IC$_{50}$ in the range 137–181 µM. In this respect, modest GST inhibitory activity was previously ascertained for **7c** and related Os(II)-EA conjugates in ovarian cancer cell lines (A2780, A2780cisR) [38]. In contrast, the Ru(II) (**7d**) and Ir(III) (**7e**) derivatives with a doubly-derivatized **EA** and flurbiprofen 2,2'-bipyridine ligand are potent GST P1 inhibitors. The iridium compound **7d** is the strongest inhibitor of GST P1 (IC$_{50}$ = 6.7 ± 0.7 µM) in the present work, more effective than **EA**. Compound **7e** exhibits significant cytotoxicity on a panel of cancer cell lines, with its biological activity benefiting from the combined action of the metal scaffold and the two enzyme inhibitors[37].

The diiron cyclopentadienyl complexes with aminocarbyne (**4a–d**) and vinyliminium (**5a–e**) ligands are either modest inhibitors of GST P1-1 or are essentially inactive, with IC$_{50}$ values in the

Table 4. GST P1-1 inhibition of ethacrynic acid and a series of organometallic compounds.

Compound	Structure[a]	IC$_{50}$ (µM ± SD)
1 Ethacrynic acid		11.3 ± 0.8
2a		57 ± 4
2b		76 ± 6
2c		24.7 ± 1.4
2d		61 ± 5
3a		235 ± 2
4a		275 ± 9

(*continued*)

Table 4. Continued.

Compound	Structure[a]	IC$_{50}$ (µM ± SD)
4b		219 ± 8
4c		113 ± 5
4d		72 ± 5
5a		83 ± 9
5b		91 ± 9
5c		46.8 ± 2.8

(continued)

Table 4. Continued.

Compound	Structure[a]	IC$_{50}$ (μM $\pm$ SD)
5d		34.0 $\pm$ 4.3
5e		30.3 $\pm$ 8.3
6a		17.4 $\pm$ 2.8
6b		165 $\pm$ 4
7a		181 $\pm$ 7
7b		152 $\pm$ 6
7c		138 $\pm$ 12

(*continued*)

Table 4. Continued.

Compound	Structure[a]	IC$_{50}$ (μM ± SD)
7d		6.7 ± 0.7
7e		12.1 ± 1.8

[a] Cationic diiron complexes as $CF_3SO_3^-$ salts; cationic Ru/Ir complexes (**3a**, **7d**, **7e**) as NO_3^- salt.

Table 5. Assessment of SIA and batch IC$_{50}$ values.

Compounds	IC$_{50}$ batch ± SD (μM)	IC$_{50}$ SIA ± SD (μM)
1	13.58 ± 0.02 [(1)]	11.3 ± 0.8
4a	226 ± 3	275 ± 9
4c	61 ± 3	113 ± 5.3
4d	33 ± 6	72 ± 5
6a	11.5 ± 0.7	17 ± 3
7e	11.6 ± 0.5	12 ± 2

IC$_{50}$ value obtained using the same batch method in reference[41].

range of 30–275 μM. The presence of (hetero)aromatic substituents on the bridging ligand is correlated with an increase in inhibitory activity, e.g. compare the IC$_{50}$ values of **4a,b,** and **5a,b** with **4c,d,** and **5c,d,e**. The thiocarbyne complex **6a**, with two cyclohexyl isocyanide ligands, is a comparatively good GST P1-1 inhibitor with an IC$_{50}$ value of 17.4 ± 2.8 μM. Notably, the introduction of a PTA ligand in **6b** dramatically impairs the ability of the compound to inhibit GST P1-1. Nevertheless, both **6a** and **6b** are effective DHFR reductase inhibitors.[45]

2.3. Validation of the SIA system

To ensure the validation of the newly developed methodology, some compounds were also analysed using a batch procedure. The IC$_{50}$ values obtained were compared with those obtained from the SIA method in Table 5 and are in reasonable agreement, showing the same trend and similar values for the active inhibitors.

The results were evaluated using the *t*-test, carried out as a bilateral coupled test. In agreement with the student's *t*-test, the tabulated *t* value (2.57), is lower than the calculated *t* value (2.3). Thus, there are no statistical differences at the confidence level of 95%[46], further confirmed by a linear correlation as described by the equation:

$$IC_{50} \ SIA \ = (1.2 \pm 0.3) \ IC_{50} \ BATCH - (12.4 \ \pm \ 30.9) \qquad (1)$$

where IC$_{50}$SIA and IC$_{50}$BATCH are, respectively, the IC$_{50}$ results acquired using the SIA and batch methods, with intercept and slope confidence limits of 95%. The predictable intercept and slope values were not considered significantly different, respectively, from 0 to 1, confirming the SIA and batch methods

agreement. The coefficient of Pearson correlation for the two methods is near 1 (∼ 0.98).

According to the goal of this study and all the advantages of using the SIA methodology such as robustness, reproducibility, versatility, computer control, and reliability, the analytical signal is obtained in 5 min whereas 8 min are required for the batch procedure. The SIA system also requires fewer materials than in batch method, i.e. 5 times less GSH solution, 1.25 times less CDNB solution, and 2.3 times less GST P1-1 solution.

4. Conclusions

An SIA system was developed to evaluate the GST P1-1 inhibition capacity of organometallic complexes with putative anticancer activity. Some of the compounds tested exhibited good inhibition profiles with the low μM range of IC$_{50}$ values and were comparable to the benchmark organic inhibitor, EA. It is therefore expected that these compounds could be useful to treat cancers where GST P1-1 is overexpressed[47–49]. The SIA method was found to be a good alternative to the batch method reducing the analysis time and the number of reagents required. Hence, the SIA method is considered an important automatic alternative for the analysis of GST P1-1 inhibitors.

Disclosure statement

The authors declare no conflict of interest.

References

1. Sau A, Pellizzari Tregno F, Valentino F, et al. Glutathione transferases and development of new principles to overcome drug resistance. Arch Biochem Biophys 2010;500: 1527–22.

2. Mathew N, Kalyanasundaram M, Balaraman K. Glutathione S-transferase (GST) inhibitors. Expert Opin Therap Pat 2006; 16:431–44.

3. Di Pietro G, Magno LA, Rios-Santos F. Glutathione S-transferases: an overview in cancer research. Expert Opin Drug Metab Toxicol 2010;6:153–70.

4. Tew KD, et al. Glutathione-associated enzymes in the human cell lines of the national cancer institute drug screening program. Mol Pharmacol 1996;50:149–59.

5. Morrow CS, Smitherman PK, Diah SK, et al. Coordinated action of glutathione S-Transferases (GSTs) and multidrug resistance protein 1 (MRP1) in antineoplastic drug detoxification. Mechanism of GST A1-1- and MRP1-associated resistance to chlorambucil in MCF7 breast carcinoma cells. J Biol Chem 1998;273:20114–20.

6. Ruzza P, Calderan A. Glutathione Transferase (GST)-activated prodrugs. Pharmaceutics 2013;5:220–31.

7. Singh S. Cytoprotective and regulatory functions of glutathione S-transferases in cancer cell proliferation and cell death. Cancer Chemother Pharmacol 2015;75:1–15.

8. Enache TA, Oliveira-Brett AM. Electrochemical evaluation of glutathione S-transferase kinetic parameters. Bioelectrochemistry 2015;101:46–51.

9. Dirican O, Kaygin P, Oguztuzun S, et al. Immunocytochemical evaluation of glutathione-s-transferase p1 enzyme in patients with rheumatoid arthritis. HLA 2019; 93:336.

10. Kool J, Eggink M, van Rossum H, et al. Online biochemical detection of glutathione-S-transferase P1-specific inhibitors in complex mixtures. J Biomol Screen 2007;12:396–405.

11. Hartwell SK, Grudpan K. Flow-based systems for rapid and high-precision enzyme kinetics studies. J Anal Methods Chem 2012;2012:450716.

12. Hansen EH. Flow-injection enzymatic assays. Analytica Chimica Acta 1989;216:257–273.

13. Silvestre CIC, Pinto PCAG, Segundo MA, et al. Enzyme based assays in a sequential injection format: a review. Analytica Chimica Acta 2011;689:160–177.

14. Gübeli T, Christian GD, Ruzicka J. Fundamentals of sinusoidal flow sequential injection spectrophotometry. Anal Chem 1991;63:2407–13.

15. Allocati N, Masulli M, Di Ilio C, et al. Glutathione transferases: substrates, inihibitors and pro-drugs in cancer and neurodegenerative diseases. Oncogenesis 2018;7:8.

16. Wani WA, Baig U, Shreaz S, et al. Recent advances in iron complexes as potential anticancer agents. New J Chem 2016;40:1063–1090.

17. Sansook S, Hassell-Hart S, Ocasio C, et al. Ferrocenes in medicinal chemistry; a personal perspective. J Organomet Chem 2020;905:121017.

18. Hwang E, Jung HS. Metal-organic complex-based chemodynamic therapy agents for cancer therapy. Chem Commun 2020;56:8332–8341.

19. Murray BS, Babak MV, Hartinger CG, et al. The development of RAPTA compounds for the treatment of tumors. Coord Chem Rev 2016;306:86–114.

20. Riedel T, Demaria O, Zava O, et al. Drug repurposing approach identifies a synergistic drug combination of an antifungal agent and an experimental organometallic drug for melanoma treatment. Mol Pharm 2018;15:116–126.

21. Riedel T, Cavin S, van den Bergh H, et al. Chemo-manipulation of tumor blood vessels by a metal-based anticancer complex enhances antitumor therapy. Sci Rep 2018;8: 10263–10263.

22. Švorc Ľ, Tomčík P, Durdiak J, et al. Analytical methods for the detection of osmium tetroxide: a review. Pol J Environ Stud 2012;21:7–13.

23. Liu Z, Sadler PJ. Organoiridium complexes: anticancer agents and catalysts. Acc Chem Res 2014;47:1174–1185.

24. Kilpin KJ, Dyson PJ. Enzyme inhibition by metal complexes: concepts, strategies and applications. Chem Sci 2013;4: 1410–1419.

25. Ang WH, De Luca A, Chapuis-Bernasconi C, et al. Organometallic ruthenium inhibitors of glutathione-S-transferase P1-1 as anticancer drugs. ChemMedChem 2007;2: 1799–806.

26. Ang WH, Parker LJ, De Luca A, et al. Rational design of an organometallic glutathione transferase inhibitor. Angew Chem Int Ed Engl 2009;48:3854–7.

27. Păunescu E, Soudani M, Martin P, et al. Organometallic glutathione S-transferase inhibitors. Organometallics 2017; 36:3313–3321.

28. Scolaro C, Bergamo A, Brescacin L, et al. In vitro and in vivo evaluation of ruthenium(II)-arene PTA complexes. J Med Chem 2005;48:4161–4171.

29. Biancalana L, Batchelor LK, Funaioli T, et al. α-diimines as versatile, derivatizable ligands in ruthenium(II) p-cymene anticancer complexes. Inorganic Chem 2018;57:6669–6685.

30. Agonigi G, Biancalana L, Lupo MG, et al. Exploring the anticancer potential of diiron bis-cyclopentadienyl complexes with bridging hydrocarbyl ligands: behavior in aqueous media and in vitro cytotoxicity. Organometallics 2020;39: 645–657.

31. Biancalana L, De Franco M, Ciancaleoni G, et al. Easily available, amphiphilic diiron cyclopentadienyl complexes exhibit in vitro anticancer activity in 2D and 3D human cancer cells through redox modulation triggered by CO release. Chem Eur J 2021;27:10169–10185.

32. Braccini S, Rizzi G, Biancalana L, et al. Anticancer diiron vinyliminium complexes: a structure–activity relationship study. Pharmaceutics 2021;13:1158.

33. Rocco D, Batchelor LK, Agonigi G, et al. Anticancer potential of diiron vinyliminium complexes. Chem Eur J 2019;25: 14801–14816.

34. Rocco D, Busto N, Pérez-Arnaiz C, et al. Antiproliferative and bactericidal activity of diiron and monoiron cyclopentadienyl carbonyl complexes comprising a vinyl-aminoalkylidene unit. Appl Organomet Chem 2020;34:e5923.

35. Marchetti F, Zacchini S, Zanotti V. C–N coupling of isocyanide ligands promoted by acetylide addition to diiron aminocarbyne complexes. Organometallics 2015;34:3658–3664.

36. Schroeder NC, Funchess R, Jacobson RA, et al. Reactions of Cp2Fe2(CO)2(.mu.-CO)(.mu.-CSR)+ bridging-carbyne complexes with nucleophiles. Organometallics 1989;8:521–529.

37. Biancalana L, Kostrhunova H, Batchelor LK, et al. Hetero-bis-conjugation of bioactive molecules to half-sandwich ruthenium(II) and iridium(III) complexes provides synergic effects in cancer cell cytotoxicity. Inorganic Chem 2021;60:9529–9541.

38. Agonigi G, Riedel T, Gay MP, et al. Arene osmium complexes with ethacrynic acid-modified ligands: synthesis, characterization, and evaluation of intracellular glutathione S-transferase inhibition and antiproliferative activity. Organometallics 2016;35:1046–1056.

39. Biancalana L, Pratesi A, Chiellini F, et al. Ruthenium arene complexes with triphenylphosphane ligands: cytotoxicity towards pancreatic cancer cells, interaction with model proteins, and effect of ethacrynic acid substitution. New J Chem 2017;41:14574–14588.

40. Biancalana L, Batchelor LK, De Palo A, et al. A general strategy to add diversity to ruthenium arene complexes with bioactive organic compounds via a coordinated (4-hydroxy-phenyl)diphenylphosphine ligand. Dalton Transactions 2017;46:12001–12004.

41. Biancalana L, Batchelor LK, Pereira SAP, et al. Bis-conjugation of bioactive molecules to cisplatin-like complexes through (2,2'-Bipyridine)-4,4'-dicarboxylic acid with optimal cytotoxicity profile provided by the combination ethacrynic acid/flurbiprofen. Chem Eur J 2020;26:17525–17535.

42. Fulci C, Rotili D, De Luca A, et al. A new nitrobenzoxadiazole-based GSTP1-1 inhibitor with a previously unheard of mechanism of action and high stability. J Enzyme Inhib Med Chem 2017;32:240–247.

43. Bräutigam M, Teusch N, Schenk T, et al. Selective inhibitors of glutathione transferase P1 with trioxane structure as anti-cancer agents. ChemMedChem 2015;10:629–39.

44. Musdal Y, Hegazy UM, Aksoy Y, et al. FDA-approved drugs and other compounds tested as inhibitors of human glutathione transferase P1-1. Chem Biol Interact 2013;205:53–62.

45. Pereira SAP, Biancalana L, Marchetti F, et al. Assessment of metal-based dihydrofolate reductase inhibitors on a novel mesofluidic platform. Sens Actuators B Chem. 2022;366:131978.

46. Miller JC, JN, Miller. Estadística para Química Analítica. Wilmington, NC: Adisson Wesley Ibroamerican; 1993.

47. McIlwain CC, Townsend DM, Tew KD. Glutathione S-transferase polymorphisms: cancer incidence and therapy. Oncogene 2006;25:1639–1648.

48. Singh RR, Reindl KM. Glutathione S-transferases in cancer. Antioxidants 2021;10:701.

49. Huang G, Mills L, Worth LL. Expression of human glutathione S-transferase P1 mediates the chemosensitivity of osteosarcoma cells. Mol Cancer Ther 2007;6:1610–9.